Korean J. Chem. Eng., 34(11), 2993-2998 (2017)
DOI: 10.1007/s11814-017-0205-z

pISSN: 0256-1115
eISSN: 1975-7220

Facile synthesis of iron-ruthenium bimetallic oxide nanoparticles on carbon nanotube composites by liquid phase plasma method for supercapacitor

Won-June Lee*, Sangmin Jeong*, Heon Lee*, Byung-Joo Kim, Kay-Hyeok An***, Young-Kwon Park****, and Sang-Chul Jung*,†**

*Department of Environmental Engineering, Sunchon National University, 255 Jungang-ro, Sunchon, Jeonnam 57922, Korea
**R&D Division, Korea Institute of Carbon Convergence Technology, 110-11 Banryong-ro, Jeonju 54853, Korea
***Department of Nano & Advanced Materials Engineering, Jeonju University, 303 Cheonjam-ro, Jeonju 55069, Korea
****School of Environmental Engineering, University of Seoul, 163 Seoulsiripdaero, Dongdaemun-gu, Seoul 02504, Korea
(*Received 11 May 2017 • accepted 24 July 2017*)

Abstract−Iron-ruthenium bimetallic oxide nanoparticles were precipitated on carbon nanotubes by liquid-phase plasma method. We also evaluated the physicochemical and electrochemical properties of prepared composite for supercapacitor electrode. Polycrystalline about 10 to 25 nm-sized bimetallic nanoparticles were evenly precipitated on the carbon nanotube (CNT) and consisted of Fe^{3+} and Ru^{4+}. Bimetallic oxide nanoparticles' composition depended on the ratio of the metal precursor concentration and standard reduction potential. The C-V area and specific capacitance of iron-ruthenium oxide nanoparticle/carbon nanotube (IRCNT) composite electrodes was higher than that of untreated CNT electrode, and increased with increasing ruthenium content. The cycling stability of IRCNT composite electrode was higher than untreated CNT electrode, especially iron element was more stable.

Keywords: Liquid Phase Plasma, Bimetallic Oxide Nanoparticle, Iron, Ruthenium, Specific Capacitance

INTRODUCTION

Energy storage has become more important than ever as interest in mobile energy devices has surged recently. Amid diverse electrochemical energy storage technologies, supercapacitors (also called electrochemical capacitors, electrical double layer capacitors, or ultracapacitors) feature high power density, simple principle and mode of construction, safety, short charging time and long cycling life [1-3]. Carbonaceous materials such as activated carbon, graphene, and carbon nanotube have been applied to electrode materials of supercapacitors because of their excellent chemical and physical properties and electrical properties [4-6]. Among these applications of carbon nanotubes (CNTs) as an electrode material for supercapacitors have had significant investigation of their micro-porous structures and electrochemical behavior [7-9].

To enhance supercapacitors' capacitive performance, many attempts have been made to fabricate composites of metal oxides with carbonaceous materials [10,11]. However, RuO_2, which has the highest conductivity and high specific capacitance among metal oxides, is limited in large scale applications because of its high cost and scarcity [12,13]. Among the metal oxides, Fe_3O_4 exhibits excellent redox activity and is abundant in nature, so that a high theoretical energy storage capacity can be obtained at relatively low cost [14].

The liquid phase plasma method provides a variety of chemical species, such as excited proton and radicals in the high density energy field. Thus, they can produce various metal and metal oxide nanoparticles in aqueous solution without additive or reducing agent [15-17]. In addition, metal and metal oxide nanoparticles can be formed on various substrates such as carbonaceous materials [18-20].

In this study, iron-ruthenium bimetallic oxide nanoparticles were precipitated on carbon nanotubes by liquid-phase plasma (LPP) method. And also, we evaluated the physicochemical and electrochemical properties of prepared IRCNT composites using various analytical instruments. Specifically, we verified the effect of initial precursor concentration ratio of iron and ruthenium. The results of as-prepared IRCNT composites with various initial concentration ratio were compared with that of bare CNT.

EXPERIMENTAL METHODS

IRCNT composites were prepared by LPP method, and a multiwalled carbon nanotube (MWCNT) (K-nanos-100P, Kumho Petro Chemical) was used as a substrate. Ruthenium (III) chloride hydrate ($RuCl_3 \cdot xH_2O$, Alfa aesar) and iron chloride tetrahydrate ($FeCl_2 \cdot 4H_2O$, Kanto Chemical Co.) were used as precursors for ruthenium and iron nanoparticles in the LPP reaction. Cetyltrimethylammonium bromide (CTAB, $CH_3(CH_2)15N(CH_3)_3Br$, Daejung Chemicals & Metals Co.) and sodium dodecyl sulfate (SDS, $C_{12}H_{25}NaO_3S$, Tokyo Chemical Industry Co.) were added together to improve the dispersibility of IRCNT composite powders in LPP reactant solutions. In this experiment, deionized water (Daejung Chemicals & Metals Co.) was used as a solvent for all the reactant aqueous solutions, and the pH of the reactant aqueous solution was controlled by using

†To whom correspondence should be addressed.
E-mail: jsc@sunchon.ac.kr
‡The authors declare that there is no conflict of interests regarding the publication of this article.

a hydrochloric acid standard solution (0.1 N HCl, Daejung Chemicals & metals Co., Ltd.).

In this experiment, iron-ruthenium oxide nanoparticles were precipitated on CNT through LPP method, and the experimental setup was similar to that used in previous studies [6,11]. Plasma in the reactant aqueous solution was generated by high frequency bipolar pulse power supply (Nano technology Inc., NTI-500W) with the power supply operating conditions: voltage 250 V, frequency 30 kHz and pulse width 5 μ. A tungsten rod (Φ2 mm, purity of 99.95%, T.TM Korea Co.) was used as the electrode and double tube type (OD: 40 mm, H: 80 mm) quartz reactor was used.

The preparing method and procedure of IRCNT composite using LPP process were as follows. $RuCl_3$ and $FeCl_2$ were completely dissolved in an aqueous solution (250 ml, pH 2) prepared by mixing DI water and 0.1 N HCl solution. To disperse the composites, CTAB and SDS were added to the total precursor at 25% molar ratio and dissolved by stirring. Only SDS was used for the reactant aqueous solution prepared with ruthenium precursor alone because CTAB was used to generate precipitate. 250 mg of CNT powder was added to this aqueous solution and stirred for 1 hour to prepare a final reactant aqueous solution. The final reactant aqueous solution was added to the LPP reactor and the IRCNT composite powder was prepared by precipitating iron-ruthenium oxide nanoparticles on CNT by LPP process for 1 hour. The IRCNT composite powders collected in aqueous solution were centrifuged and washed three times to remove unreacted materials and vacuum dried at 353 K for 48 hours.

The chemical composition and dispersibility of IRCNT composites prepared by LPP method were analyzed by field emission scanning electron microscope (FESEM, JSM-7100F, JEOL) and the morphology and size of nanoparticles on CNT surface were observed by high resolution field emission transmission electron microscope HR-FETEM, JEM-2100F, JEOL). The emission spectra in the LPP reaction were confirmed using an optical emission spectrometer (AvaSpec-3648, Avantes), and X-photoelectron spectroscopy (XPS, K-Alpha system, Thermo Scientific Inc.) was used to analyze the chemical structure of IRCNT composite. To evaluate electrochemical properties of IRCNT composites, a coin cell type battery was prepared. Coin cells were prepared by mixing active material (IRCNT composite powders) : conducting agent (Super-P carbon black, TIMCAL graphite & carbon com.) : Binder (Polyvinylidene fluoride) in 80 : 10 : 10 wt%. 1 M H_2SO_4 solution was used as the electrolyte and 150 μm glass felt was used as the separator. The C-V curves were measured by cyclic voltammetry at an actuation voltage of 0.1 to 0.8 V, a current density of 0.001 A/cm^2, and a scan rate of 10 mV/s. The electrochemical properties were measured by a VSP potentiostat (Bio-logic Sci. Ins.). For each sample, three coin cells were used with performance of electrochemical test.

RESULTS AND DISCUSSION

To determine what kind of chemically active species were produced in this LPP reactant solution, we observed by using optical emission spectra (OES), and the results are shown in Fig. 1. Fig. 1 shows emission spectra generated from (a) pure water, (b) iron reactant solution, (c) ruthenium reactant solution, and (d) the iron and

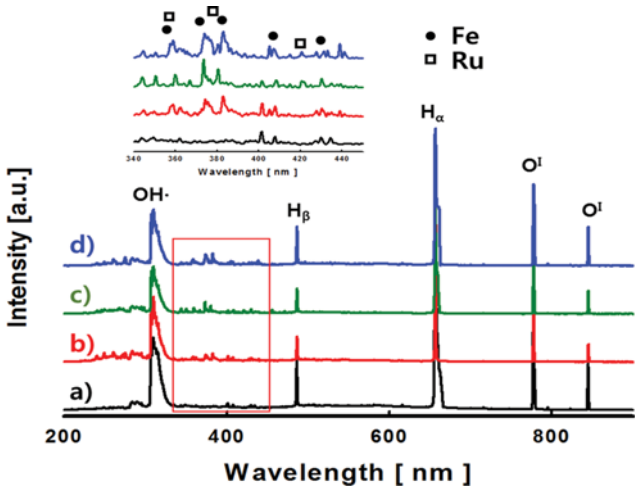

Fig. 1. Spatially and temporally integrated emission spectra for the pulsed electric discharge in iron-ruthenium chloride reactant solution: (a) Pure water, (b) iron reactant solution, (c) ruthenium reactant solution, (d) iron and ruthenium reactant solution.

ruthenium reactant solution. In pure water, strong molecular bands of the hydroxyl radical OH were observed at 309 nm and excited states of atomic hydrogen were observed at 656 nm and 486 nm. In addition, atomic oxygen was observed at 777 nm and 844 nm. Iron and ruthenium precursor solutions showed intense concentrations of iron and ruthenium metal peaks in the range of 340 to 450 nm. On the other hand, iron and ruthenium metal peaks were also observed in the mixed solution of iron and ruthenium precursor (Fig. 1(d)). More specifically, atomic iron (Fe I Ground state electron configuration $1s^2 2s^2 2p^6 3s^2 3p^6 3d^6 4s^2\ ^5D^4$) was observed at 344.0, 358.1, 373.7, 382.0, 404.5, and 438.3 nm, and atomic ruthenium (Ru I Ground state electron configuration $1s^2 2s^2 2p^6 3s^2 3p^6 3d^{10} 4s^2 4p^6 4d^7 5s\ 5F_5$) was observed at 349.8, 373.0, 379.9, and 419.9 nm [21].

The morphology and dispersibility of the precipitated iron-ruthenium oxide nanoparticles on the CNT surface were investigated using FESEM. Upper left corner in the Fig. 2 shows the real image of the IRCNT composite powder prepared by the LPP method. And, shows together the mapping images of ruthenium, iron, and oxygen elements in IRCNT composite powders. The IRCNT composite powder shows an irregular spherical shape, and the scale bar in microscope image is 10 μm. The ruthenium, iron, and oxygen elements are mapped to green, red, and blue dots, respectively, and all elements are uniformly dispersed in the IRCNT composite. These results indicate that the particles produced in present study are metal oxide nanoparticles and that can be uniformly dispersed by the LPP process. The metal ions (Ru^{3+} and Fe^{2+}) in the reactant solution are dwindled by the electrons and excited hydrogen generated in the LPP reaction, and they are converted into metal oxide nanoparticles by hydroxyl radicals and excited oxygen [16,17].

The chemical composition of IRCNT composites prepared by LPP process using reactant solutions with different initial concentration of precursors was measured by energy dispersive spectroscopy (EDS) in FESEM. Table 1 shows the chemical composition of CNT and IRCNT composites prepared at different initial precursors

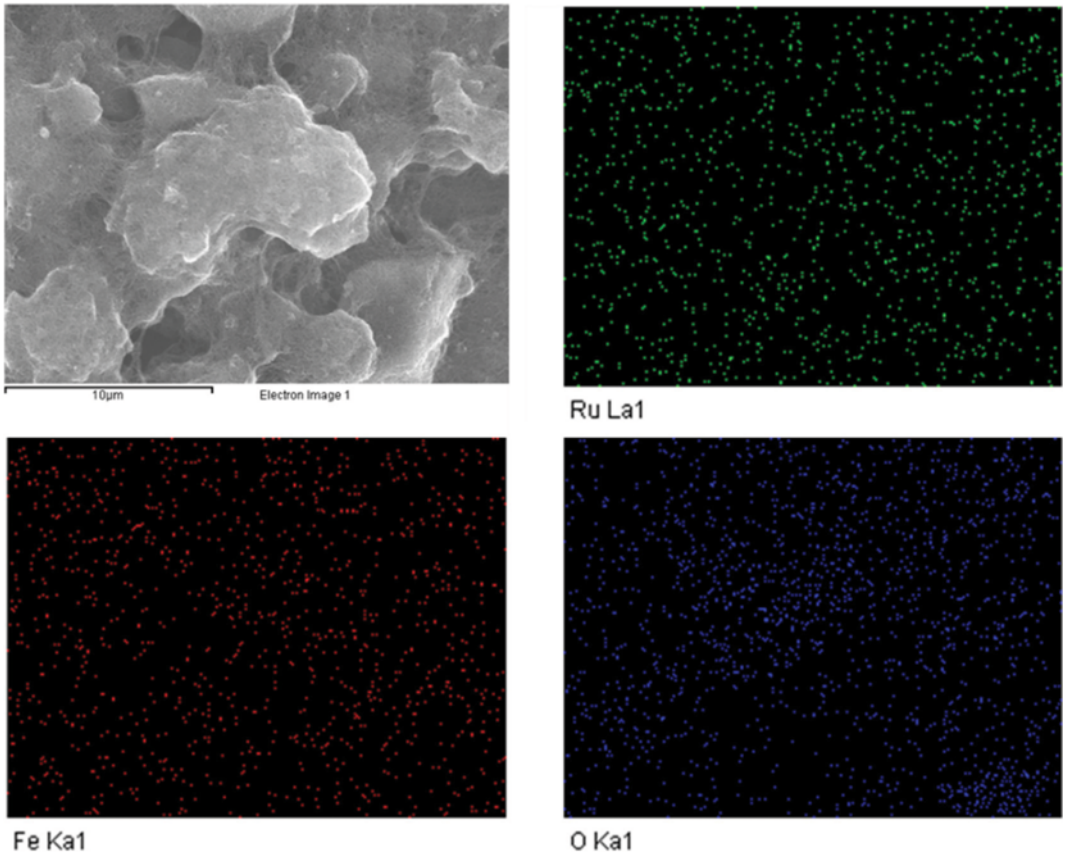

Fig. 2. FESEM real image and EDS elemental maps of IRCNT composite powders prepared by LPP method.

Table 1. Chemical composition of IRCNT composites synthesized under different conditions of initial concentration of precursors of LPP reactant solution

Samples	Concentration (mM)		Carbon		Oxygen		Ruthenium		Iron	
	Ru	Fe	wt%	at%	wt%	at%	wt%	at%	wt%	at%
CNT	0	0	92.68	94.40	7.32	5.60	0.00	0.00	0.00	0.00
IRCNT-1	1	0	89.33	92.94	8.24	6.82	1.94	0.24	0.00	0.00
IRCNT-2	0.7	3	89.56	93.00	8.49	6.74	1.43	0.18	0.37	0.08
IRCNT-3	0.5	5	89.82	93.13	8.66	6.60	1.09	0.13	0.62	0.14
IRCNT-4	0.3	7	89.93	93.21	9.04	6.45	0.57	0.07	1.21	0.27
IRCNT-5	0	10	90.08	93.22	8.73	6.41	0.00	0.00	1.68	0.37

concentration of reactant solution. It can be seen that the CNT used as a substrate in this study contains 5.6 at% of oxygen. At ruthenium precursor (IRCNT-1) alone, 0.24 at% of ruthenium was precipitated on CNT, and when only iron precursor (IRCNT-5) was used, 0.37 at% of iron precipitated on CNT. The concentrations of ruthenium precursor (1 mM) and iron precursor (10 mM) used in the experiment were significantly different, but the amounts precipitated were similar. This is because the reduction potential of ruthenium and iron is different due to the standard reduction potentials [17]. One side, IRCNT composites prepared from reactant solutions prepared by mixing precursors showed that the higher the precursor concentration, the more precipitated. Also, the content of oxygen increased with increasing amount of ruthenium precipitated in CNT.

HR-FETEM was used to observe the morphology and size of the nanoparticles precipitated on the CNT surface by the LPP process. Fig. 3(a) is an image of the IRCNT composite prepared with the IRCNT-3 reactant solution at low magnification (×15,000). CNTs that are interwoven with each other are observed, and nanoparticles of about 10 to 26 nm in size are observed on the CNTs. Fig. 3(b) shows an oval-shaped nanoparticle with an image observed at high magnification (×500,000). Also, in the upper right region, the electron discharge (ED) pattern of nanoparticles is represented. This pattern does show little spots and circles, indicating that nanoparticles are amorphous particles.

In this study, line mapping was performed using HR-FETEM to investigate the chemical composition of nanoparticles precipitated on the CNT surface using the LPP process. Fig. 4(a) shows

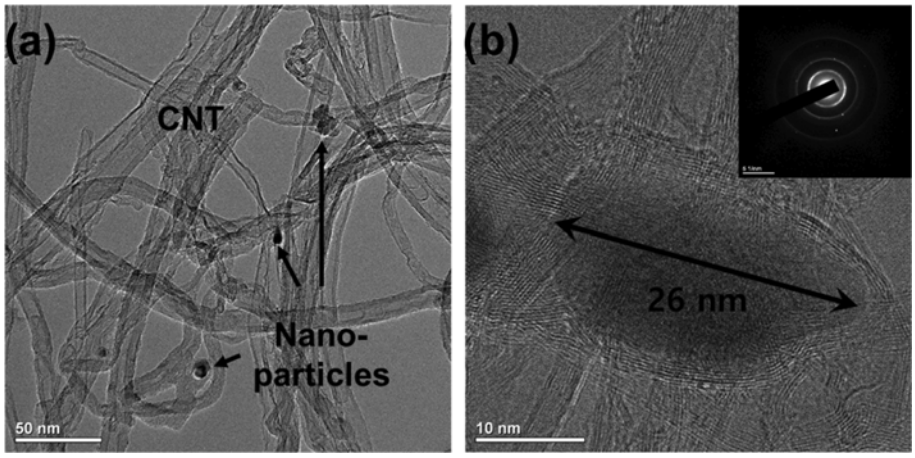

Fig. 3. HR-FETEM images of IRCNT-3 composite prepared by LPP method: (a) low magnification (×15,000), and (b) high magnification (×500,000) including ED pattern.

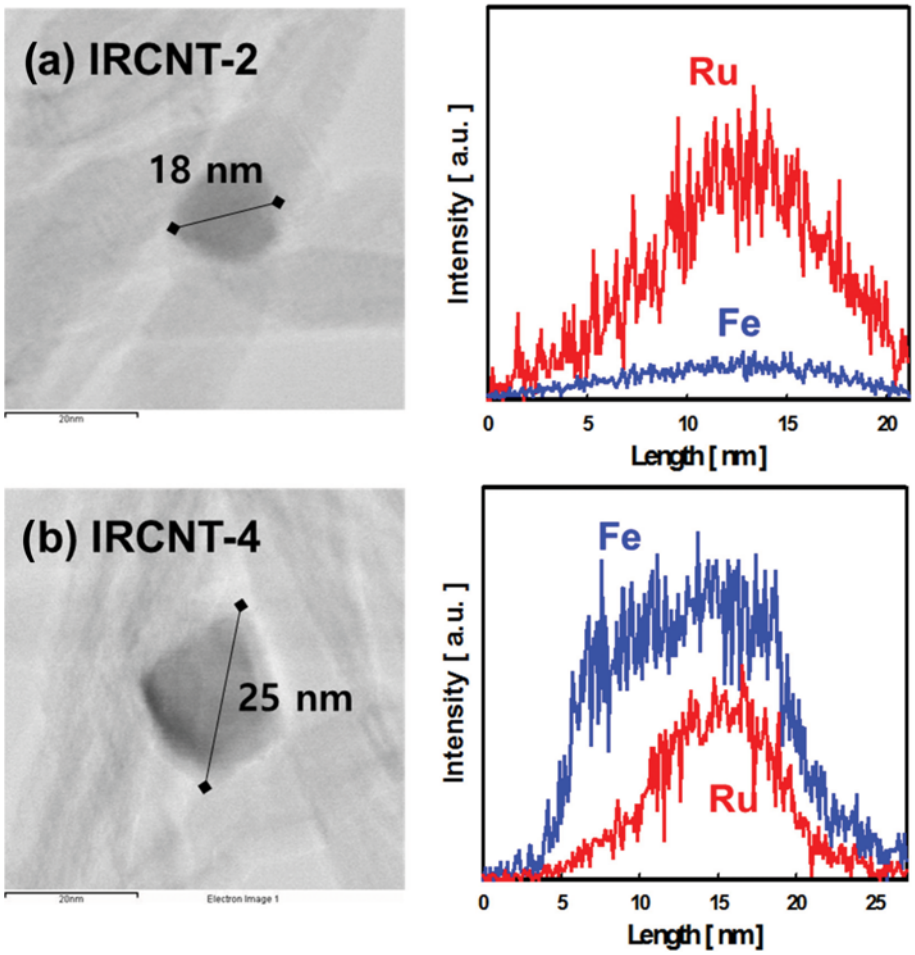

Fig. 4. HR-TEM image and EDS line scanning profile of IRCNT composites prepared by LPP method with different initial precursor concentration: (a) IRCNT-2 and (b) IRCNT-4.

the TEM image and line mapping of IRCNT-2, and 4(b) shows IRCNT-4s image and line mapping. All of the nanoparticles shown in Fig. 4 were mixed with iron and ruthenium elements. These results suggest that the nanoparticles precipitated on the CNT surface by the LPP method are bimetallic oxide nanoparticles. The IRCNT-2 particle size was 18 nm and the IRCNT-4 particle size was 25 nm. The bimetallic oxide nanoparticle (IRCNT-2) precipitated as a reactant solution with a high initial concentration of ruthe-

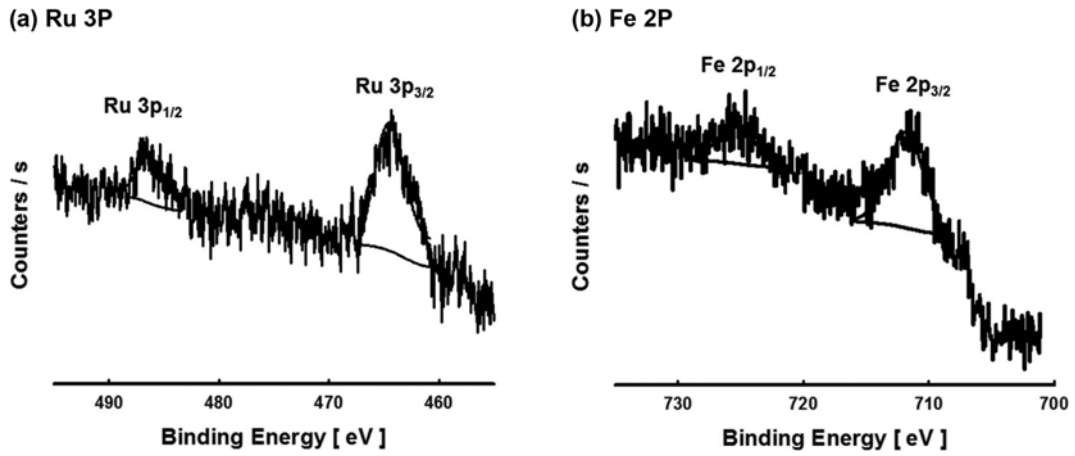

Fig. 5. High resolution XPS spectrum for the (a) Ru 3p region and (b) Fe 2p region of IRCNT-3 composite prepared by LPP method.

nium precursor can be seen from the line mapping (Fig. 4(a)) that the ruthenium component is higher than iron. On the other hand, the bimetallic oxide nanoparticle (IRCNT-4) precipitated as a reactant solution with an initial concentration of iron precursor can be seen from the line mapping (Fig. 4(b)) that the iron content is higher than ruthenium. From these results, the precursor concentration in the aqueous solution influences the composition of the produced bimetallic particles. The Ru^{3+} and Fe^{2+} ions dissociated in the reactant solution are reduced to metal particles by the electrons and reducing agents generated through LPP reaction. Therefore, the composition of bimetallic particles is driven by the precursor concentration in aqueous solution and the intensity of the reduction potential of precursor element. These results are the same as the chemical composition of IRCNT composites shown in Table 1.

High resolution XPS was used to investigate the chemical state of bimetallic oxide nanoparticles formed by LPP method on CNT surface. Fig. 5 shows the narrow-range XPS spectra of the IRCNT-3 composite. Fig. 5(a) shows the spectrum in the Ru 3p region, and the binding energy (BE) of 464.2 eV and 486.2 eV confirmed Ru $3p_{3/2}$ and Ru $3p_{1/2}$ peaks. From this XPS analysis, it can be seen that ruthenium element exists as Ru^{4+} state [22]. In addition, the spin orbit splitting (SOS) of $3p_{3/2}$ and $3p_{1/2}$ peaks is 22.0 eV and RuO_2 type is maintained [23]. Fig. 5(b) shows the spectrum in the Fe 2p region and peaks due to Fe $2p_{3/2}$ and Fe $2p_{1/2}$ were noticed at 711.9 eV and 725.4 eV, respectively. Here, the SOS was calculated to be 13.5 eV, which indicates that the Fe_2O_3 structure having Fe^{3+} valence was obtained.

In this study, IRCNT composites prepared by the LPP method were applied to supercapacitor electrodes. To evaluate the electrochemical properties of IRCNT composite electrodes, three half-coin cell type batteries were prepared. All of the electrochemical properties presented here are the average of three measurements. The C-V curves of electrodes made with untreated CNT and IRCNT composites were measured using the cyclic-voltammetry method (Fig. 6). At this time, the measured voltage was 0.1 to 0.8 V and the scan rate was maintained at 10 mV/s. In the C-V curve measurement, all cells showed a rectangular shape. In addition, all IRCNT composites showed increased C-V area and initial response compared to untreated CNT. The C-V curve area of IRCNT-5 composite electrodes prepared using only iron precursors were slightly increased compared to untreated CNT. In particular, the C-V curve

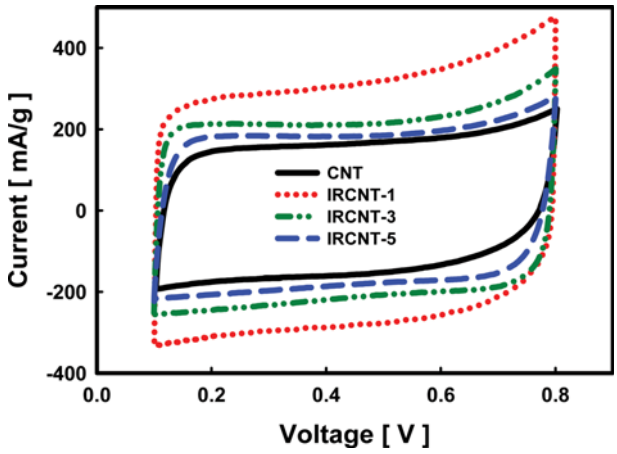

Fig. 6. C-V curves of IRCNT composites preparede by LPP method with different initial concentration of precursor.

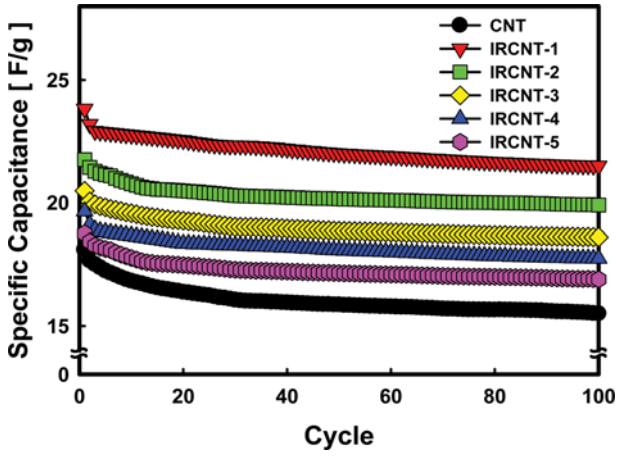

Fig. 7. Changes in specific capacitance for untreated CNT and IRCNT composite electrodes as a different initial precursor concentration over rotational cycles of charge and discharge.

area of the IRCNT-1 composite electrode prepared using only the ruthenium precursor was the largest, and the C-V curve area tended to increase with increasing ruthenium composition.

Fig. 7 shows the results of observing the change of specific capacitance when the cells prepared by IRCNT composites were repeatedly charged and discharged 100 times. The initial specific capacitance of the cell prepared with untreated CNT was 18.10 F/g, and after 100 cycles it decreased to 15.50 F/g and maintained 85.7%. All IRCNT composite electrode cells prepared by LPP process showed higher specific capacitance value than untreated CNT. Especially, higher specific capacitance was observed with higher ruthenium composition. The initial specific capacitance value of the cell (IRCNT-1) was prepared with only ruthenium precursor was 21.49 F/g, and after 100 cycles, the specific capacitance was maintained at 90.3%. The initial specific capacitance value of cell (IRCNT-5) using only iron precursor was 16.90 F/g, and after 100 cycles, 91.5% specific capacitance was maintained. From these results, the cycling stability of IRCNT composite electrodes prepared by LPP process is higher than untreated CNT. Especially, iron element is more stable. The initial specific capacitances of the cells (IRCNT-2, 3 and 4) prepared using bimetallic oxide nanoparticle composites were 19.90 F/g, 18.60 F/g and 17.74 F/g; after 100 cycles, the specific capacitance values decreased by 9.65, 9.37 and 9.14%, respectively.

CONCLUSION

A supercapacitor electrode was formed by precipitating iron-ruthenium bimetallic oxide nanoparticles on carbon nanotube practicing a liquid phase plasma process. Polycrystalline 10 to 25 nm-sized bimetallic oxide nanoparticles were precipitated evenly on the CNT surface. The composition of the bimetallic oxide nanoparticles depended on the ratio of the metal precursor concentration and standard reduction potential. By XPS analysis, it is noticeable that the bimetallic oxide nanoparticles precipitated on the CNT surface were largely composed of Fe^{3+} and Ru^{4+}. The C-V area and specific capacitance of IRCNT composite electrodes was higher than that of untreated CNT electrode, and increased with increasing ruthenium content. The cycling stability of IRCNT composite electrode is higher than untreated CNT electrode, especially iron element is more stable.

ACKNOWLEDGEMENTS

This paper was supported by Sunchon National University Research Fund in 2017.

REFERENCES

1. A. Burke, *J. Power Sources*, **91**, 37 (2000).
2. Z. B. Lei, N. Christov and X. S. Zhao, *Energy Environ. Sci.*, **4**, 1866 (2011).
3. Z. Chen, Y. C. Qin, D. Weng, Q. F. Xiao, Y. T. Peng, X. L. Wang, H. X. Li, F. Wei and Y. F. Lu, *Adv. Funct. Mater.*, **19**, 3420 (2009).
4. R. N. Reddy and R. G. Reddy, *J. Power Sources*, **124**, 330 (2003).
5. C. Wan, K. Azumi and H. Konno, *Electrochim. Acta*, **52**, 3061 (2007).
6. H. Lee, S. H. Park, S. J. Kim, Y. K. Park, B. J. Kim, K. H. An, S. J. Ki and S. C. Jung, *Int. J. Hydrogen Energy*, **40**, 754 (2015).
7. K. H. An, W. S. Kim, Y. S. Park, J. M. Moon, D. J. Bae, S. C. Lim, Y. S. Lee and Y. H. Lee, *Adv. Funct. Mater.*, **11**, 387 (2001).
8. N. Venugopal and W. S. Kim, *Korean J. Chem. Eng.*, **32**, 1918 (2015).
9. Y. Zhang, L. Li, H. Su, W. Huang and X. Dong, *J. Mater. Chem. A*, **3**, 43 (2015).
10. Y. Shan and L. Gao, *Mater. Chem. Phys.*, **103**, 206 (2007).
11. H. Lee, B. H. Kim, Y. K. Park, K. H. An, Y. J. Choi and S. C. Jung, *Int. J. Hydrogen Energy*, **41**, 7582 (2016).
12. T. C. Liu, W. G. Pell and B. E. Conway, *Electrochim. Acta*, **42**, 3541 (1997).
13. J. F. Xie, X. Sun, N. Zhang, K. Xu, M. Zhou and Y. Xie, *Nano Energy*, **2**, 65 (2013).
14. H. Lee, S. H. Park, S. J. Kim, Y. K. Park, K. H. An, B. J. Kim and S. C. Jung, *J. Nanomater.* (2014), DOI:10.1155/2014/132032.
15. H. Lee, S. H. Park, S. J. Kim, Y. K. Park, B. H. Kim and S. C. Jung, *Microelectron. Eng.*, **126**, 153 (2014).
16. S. H. Sun and S. C. Jung, *Korean J. Chem. Eng.*, **33**, 1075 (2016).
17. S. J. Lee, H. Lee, K. J. Jeon, H. Park, Y. K. Park and S. C. Jung, *Nanoscale Res. Lett.*, **11**, 344 (2016).
18. D. J. Lee, S. J. Kim, J. Lee, H. Lee, H. G. Kim and S. C. Jung, *Sci. Adv. Mater.*, **6**, 1599 (2014).
19. H. Lee, S. J. Kim, K. H. An, J. S. Kim, B. H. Kim and S. C. Jung, *Adv. Mater. Lett.*, **7**, 98 (2016).
20. B. H. Kim, Y. K. Park, K. H. An, H. Lee and S. C. Jung, *Sci. Adv. Mater.*, **8**, 1769 (2016).
21. J. E. Sansonetti and W. C. Martin, *J. Phys. Chem. Ref. Data*, **34**, 1559 (2005).
22. K. C. Park, I. Y. Jang, W. Wongwiriyapan, S. Morimoto, Y. J. Kim, Y. C. Jung, T. Toya and M. Endo, *J. Mater. Chem.*, **20**, 5345 (2010).
23. A. Salomonsson, R. M. Petoral Jr., K. Uvdal, C. Aulin, P. O. Kall, L. Ojamae, M. Strand, M. Sanati and A. L. Spetz, *J. Nanoparticle Res.*, **8**, 899 (2006).